C_4 grasses adapted to low precipitation habitats show traits related to greater mesophyll conductance and lower leaf hydraulic conductance

VARSHA PATHARE[1], Balasaheb Vitthal Sonawane[1], Nuria Koteyeva[2], and Asaph B. Cousins[1]

[1]Washington State University
[2]V. L. Komarov Botanical Institute of Russian Academy of Sciences

April 29, 2020

Abstract

In habitats with low water availability, a fundamental challenge for plants will be to maximize photosynthetic C-gain whilst minimizing transpirational water-loss. This tradeoff between C-gain and water-loss can in part be achieved through the coordination of leaf-level photosynthetic and hydraulic traits. To test the relationship of photosynthetic C-gain and transpirational water-loss we grew under common growth conditions 18 C_4 grasses adapted to habitats with different mean annual precipitation (MAP) and measured leaf-level structural and anatomical traits associated with mesophyll conductance (g_m) and leaf hydraulic conductance (K_{leaf}). The C_4 grasses adapted to lower MAP showed greater mesophyll surface area exposed to intercellular air spaces (S_{mes}) and adaxial stomatal density (SD_{ada}) which supported greater g_m. These grasses also showed greater leaf thickness and vein-to-epidermis distance which may lead to lower K_{leaf}. Collectively, these leaf traits associated with g_m and K_{leaf} scaled positively with photosynthetic rates (A_{net}) and leaf-level water-use efficiency (WUE) with low MAP adapted grasses exhibiting greater A_{net} and WUE. In summary, we identify a suite of leaf-level traits that appear important for adaptation of C_4 grasses to habitats with low MAP and may be useful to identify C_4 species showing greater A_{net} and WUE in drier conditions.

Introduction

C_4 photosynthesis has evolved independently in multiple grass lineages (Grass Phylogeny workshop 2012) thus leading to remarkable structural, anatomical and physiological trait diversity (Christin *et al.* , 2013). Studies suggest that this trait diversity among the C_4 species could be attributed to their adaptation to different environmental variables like temperature, fire frequency and precipitation (Edwards & Smith, 2010; Visser*et al.* , 2012; Zhou *et al.* , 2018). In general, C_4 species mostly occupy the lower latitudes where light availability and temperature likely do not strongly limit photosynthesis and growth (Pearcy & Ehleringer, 1984). Instead, precipitation may be an important factor affecting trait diversity in C_4species; particularly, in traits associated with photosynthetic C-gain and transpirational water-loss (Edwards & Still, 2008; Osborne & Sack, 2012; Zhou *et al.* , 2018). During the adaption to habitats with low water availability, a fundamental challenge for plants will be to maintain photosynthetic C-gain while minimizing transpirational water-loss associated with high evaporative demand. This tradeoff could be achieved partly through coordination of leaf-level photosynthetic and hydraulic traits (Brodribb *et al.* , 2007; Nardini & Luglio, 2014; de Boer *et al.* , 2016). However, the extent of variation and coordination among these traits, particularly those associated with internal CO_2-diffusion conductance (g_m) and leaf hydraulic conductance (K_{leaf}), has not been well studied in C_4 species adapted to habitats with varying water availabilities (Osborne & Sack, 2012; Liu & Osborne, 2015; Taylor *et al.* , 2018). Although this type of trait variation and coordination has been studied in C_3 plants there could be significant differences in C_4 plants due to their unique anatomy and physiology (Kocacinar & Sage, 2003; Osborne & Sack, 2012; Ocheltree *et al.* , 2016; Zhou *et al.* , 2018).

During adaptation to drier habitats, species can exhibit several leaf-level structural and anatomical traits that can help maximize photosynthetic C-gain at a given water-loss (Wright *et al.* , 2001; Galmés *et al.* , 2012; Ivanova *et al.* , 2018b). For instance, presence of greater stomatal densities and amphistomaty (stomata on both leaf surfaces) in drier habitats, is beneficial as it reduces the role of boundary layer conductance in constraining leaf gas exchange, helps optimize leaf interior water status for CO_2 transport by reducing temperature gradients, and helps reduce the effective leaf thickness by decreasing the CO_2-diffusion pathlength (Galmés *et al.* , 2012; Muir, 2018; Drake *et al.* , 2019; Muir, 2019; Pathare *et al.* , 2020). Greater stomatal densities and smaller stomatal size in drier habitats may increase theoretical maximum stomatal conductance (g_{max}) which in turn could help plants maximize C-gain particularly during intermittent periods of water availability (Hetherington & Woodward, 2003; Franks & Beerling, 2009). Furthermore, mesophyll traits like S_{mes} and S_c - the parameters that characterize exchange surfaces for CO_2, negatively correlated with water availability in the C_3 species of European steppe plant communities and were suggested as indicators of increasingly drought adapted steppe plants (Ivanova *et al.* , 2018a; Ivanova *et al.* , 2018b). These structural and anatomical adaptations could help maximize internal CO_2-diffusion conductance (g_m), at a given stomatal conductance (g_{sw}), thus leading to greater photosynthetic rates (A_{net}) as well as leaf-level water-use efficiency (WUE) in species adapted to drier habitats (Flexas *et al.* , 2008; Flexas *et al.* , 2013; Ivanova *et al.* , 2018a; Ivanova *et al.* , 2018b). However, very few studies, mostly based on C_3 species, have investigated the leaf-level structural and anatomical traits associated with g_m that could be a characteristic of plant adaptation to drier habitats (Ivanova *et al.* , 2018a; Ivanova*et al.* , 2018b). Alternatively, even though C_4species can successfully occupy drier and warmer habitats and form grasslands over vast areas globally, there is a little information about leaf-level structural and anatomical traits that influence photosynthetic C-gain and water-use in these species. Specifically, we are unaware of any studies that have investigated the relationship of g_m and associated anatomical traits in diverse C_4 species from habitats with different water availability. In a previous study (Pathare *et al.* , 2020) we investigated the structural and anatomical determinants of g_m in diverse C_4 grasses and found that, leaf thickness, adaxial stomatal densities (SD_{ada}), stomatal ratio (SR) and S_{mes} had a positive effect on g_m. In the current study, our aim is to determine if the variation in above traits among the C_4 species could be related to adaptation to habitats with different water availabilities. Our first hypothesis (H1) is that, C_4 grasses adapted to lower MAP will show leaf anatomical traits associated with greater g_m in order to maximize photosynthetic C-gain.

Though we hypothesized a greater g_m in C_4 grasses adapted to low MAP (H1), one would expect an increase in water cost relative to photosynthetic C-gain, because g_m and associated traits have been shown to scale positively with leaf hydraulic conductance (K_{leaf}) in C_3 species (Flexas *et al.* , 2013; Xiong *et al.* , 2015; Xiong *et al.* , 2017; Drake *et al.* , 2019). K_{leaf} is an important trait associated with leaf water transport and represents the conductance to flow of water from the leaf petiole through the xylem, then through the bundle sheath and finally through the mesophyll to the site of evaporation (Sack & Holbrook, 2006; Noblin *et al.* , 2008; Buckley, 2015; Buckley *et al.* , 2015). Though K_{leaf} is partitioned between the xylem (K_x) and the outside xylem pathways (K_{ox}), changes to K_{ox} are expected to have the largest effects on K_{leaf} (Buckley *et al.* , 2015; Scoffoni *et al.* , 2017; Xiong & Nadal, 2019). Consequently, leaf-level anatomical traits that influence K_{ox} such as leaf thickness, vein-to-epidermis distance (VED), vein length per unit of leaf area (VLA) and bundle sheath and mesophyll traits are expected to have a significant effect on K_{leaf} (Griffiths *et al.* , 2013; Sack *et al.* , 2013; Buckley *et al.* , 2015). For instance, greater leaf thickness and VED, if associated with low VLA, may increase the length of post-venous water path thus leading to lower K_{leaf}. Alternatively, greater VLA in thinner leaves may increase K_{leaf} by providing additional parallel flow paths through the vein system and decreasing the horizontal pathlength from veins to sites of evaporation (Brodribb *et al.* , 2007; Sack & Scoffoni, 2013; Buckley *et al.* , 2015; Drake *et al.* , 2019). Furthermore, greater bundle sheath (BS) surface area ratio, lower BS cell wall thickness (BS_{CW}) and BS exposed to intercellular air spaces (BS_{ias}) and greater S_{mes} may all enhance K_{leaf} (Buckley*et al.* , 2015; Caringella *et al.* , 2015; Xiong *et al.* , 2017; Scoffoni *et al.* , 2018). Investigating the coordination of above traits related to water-use with traits related to C-gain will provide insights into the water cost associated with photosynthetic C-gain in C_4 species adapted to habitats with varying water availabilities.

Previous studies on C_3 species have shown a strong positive linkage of K_{leaf} with g_{sw} and hence A_{net} (Brodribb *et al.* , 2007; Brodribb & Feild, 2010; Flexas *et al.* , 2013; Scoffoni *et al.* , 2016). Additionally, the few studies that address the coordination of K_{leaf} and g_m show that these two traits scale positively with each other in C_3 species as they share some structural and anatomical traits that form the mechanistic basis for their coordination independent of g_{sw} (Flexas*et al.* , 2013; Xiong *et al.* , 2015; Xiong *et al.* , 2017) but see (Théroux-Rancourt *et al.* , 2014; Loucos *et al.* , 2017; Wang *et al.* , 2018). For example, S_{mes}positively correlates with both g_m and K_{leaf} (Flexas *et al.* , 2013; Xiong *et al.* , 2015; Xiong *et al.* , 2017) , since greater S_{mes}increases the number of parallel pathways for CO_2-diffusion inside mesophyll cells (Evans *et al.* , 2009) as well as the evaporating surface area for water thus increasing g_m and K_{leaf} respectively (Sack & Scoffoni, 2013; Xiong *et al.* , 2017). In summary, the positive correlation of K_{leaf} with $g_m$implies a greater water cost associated with greater C-gain, which could be detrimental in drier conditions where using water efficiently will be important for plant growth and fitness. Hence, a safer strategy for plants is to maintain lower K_{leaf} in drier conditions at the cost of A_{net} and growth rates (Sinclair *et al.* , 2008; Nardini & Luglio, 2014; Scoffoni *et al.* , 2016). However, these generalizations are mostly based on studies of C_3 species. It is unclear if these results would apply to C_4 grasses that are adapted to relatively drier habitats and may show different coordination between the traits associated with photosynthetic C-gain and transpirational water loss (Kocacinar & Sage, 2003; Ocheltree *et al.* , 2016; Zhou *et al.* , 2018). Increased bundle sheath size and vein densities are the anatomical precursors for evolution of C_4 species from their C_3 ancestors that led to higher K_{leaf} in the C_4 species compared to C_3 species. (Osborne & Sack, 2012; Christin *et al.* , 2013; Griffiths *et al.* , 2013). At the same time, evolution of carbon concentrating mechanism in C_4 species allows maintenance of lower g_s and higher leaf water potential. Hence, it has been proposed that once the C_4 species evolved, subsequent selection for traits leading to greater K_{leaf} would be lessened particularly during adaptation to drier habitats and there could be a decoupling between K_{leaf} and A_{net} within the C_4 lineages (Zhou *et al.* , 2018). Consequently, in contrast to C_3 species, maintaining greater K_{leaf} in order to achieve higher A_{net}may not be necessary in C_4 species and K_{leaf} may be uncoupled from g_{sw}, A_{net} (Kocacinar & Sage, 2003; Ocheltree *et al.* , 2016) and potentially g_m. However, to our knowledge, there have been no previous studies on the correlation of g_m with K_{leaf} or traits associated with K_{leaf} in C_4 species adapted to habitats with diverse MAP. Building knowledge upon previous evidences, we hypothesized (H2) that C_4 species adapted to habitats with low MAP will show traits associated with lower K_{leaf} that will maximize photosynthetic C-gain at a given water loss.

To test the above hypotheses, we selected 18 C_4 grasses that varied significantly in structural and anatomical traits (Pathare*et al.* , 2020). The grasses were grown under common growth conditions and abundant water and nutrient supply which avoids the influence of environmental conditions on traits and thus helps identify the differences that could be a result of species adaptation to their habitat of evolution or common occurrence (Reich *et al.* , 2003). We measured important leaf-level structural and anatomical traits associated with photosynthetic C-gain and g_m and transpirational water-loss and K_{leaf} in 18 diverse C_4 grasses. There is a significant knowledge gap about how C_4-g_m variability relates with habitat climate variables like MAP largely because of the lack of techniques to estimate C_4-g_m in field as well as laboratory conditions. However, the recent developments provide the opportunity to estimate C_4-g_m under laboratory conditions and thus investigate the relationship of habitat climate variables with g_m in diverse C_4species. Here, we use a recently developed method, based on modeling of leaf oxygen isotope discrimination during photosynthesis, to estimate g_m in 18 diverse C_4 grasses (Barbour*et al.* , 2016; Ubierna *et al.* , 2017; Ogee *et al.* , 2018). K_{leaf} was estimated from anatomical traits like leaf thickness, vein-to-epidermis distance (VED) and vein-to-vein distance (IVD) as recently described by de Boer *et al* ., (2016) using the semi-empirical model of Brodribb *et al* ., (2007).

Material and Methods

Plant material and growth conditions

Eighteen C_4 grasses (Table 1) representing the three classical biochemical subtypes and 8 evolutionary lineages were selected for this study. However, the aim of our study was not to look at subtype or lineage effect but to maximize leaf physiological, structural and anatomical trait diversity. Each species was given a unique identification number (Table S1) for presentation in Fig. 2-5 and S5-S8.

As previously described by Pathare *et al* ., (2020) plants were grown in 3-L free drainage pots in a controlled environment growth chamber (model GC-16; Enconair Ecological Chambers Inc., Winnipeg, MB, Canada). The photoperiod was 14 h including a 2 h ramp at the beginning and end of the light period. Light and dark temperatures were maintained at 26 and 22 °C, respectively. Light was provided by 400-W metal halide and high-pressure sodium lamps with maximum photosynthetic photon flux density (PPFD) of ca. 1000 μmol photons $m^{-2}s^{-1}$ at plant height. One individual per species was grown per pot in a Sunshine mix LC-1 soil (Sun Gro Horticulture, Agawam, MA, USA) with 6-7 replicate pots per species. The plants were irrigated daily to pot saturation and fertilized twice a week with Peters 20-20-20 (2.5 g L^{-1}). Plants were supplemented with Spring 330 iron chelate (BASF, Ludwigshafen, Germany) and Scott-Peters Soluble Trace Element Mix (The Scotts Co., Marysville, OH, USA) once a week at concentrations of 10 mg L^{-1}. Pot locations were randomized daily within the growth chamber.

Habitat mean annual precipitation and mean annual temperature

The global distribution data for the geo-referenced species was extracted from the Global Biodiversity Information Facility (GBIF; http: //www.gbif.org/) site using the *gbif* function in R package (version 3.5.2) *dismo* (Hijmans & van Etten, 2012). Values for mean annual temperature (MAT) and mean annual precipitation (MAP) from 1970 to 2000 for all geo-referenced localities for each species were extracted from the WorldClim dataset (http: //www.worldclim.org/) using the *extract* function in R package *raster* (Hijmans & van Etten, 2012). The values were then averaged as the MAT and MAP value for a given species.

Measurement of physiological traits and mesophyll conductance

The measurements of net photosynthetic rates (A_{net}), stomatal conductance to water vapor (g_{sw}), intercellular CO_2 concentrations (C_i), transpiration (E), intrinsic WUE (A_{net}/ g_{sw}), instantaneous WUE (A_{net}/E) and mesophyll conductance to CO_2 (g_m) were previously described in Pathare *et al* ., (2020). Briefly, isotopologs of CO_2 and H_2O were measured using the LI-6400XT infrared gas analyzer (LiCor, Lincoln, NE, USA) coupled to a tunable diode laser absorption spectroscope (TDLAS, model TGA 200A, Campbell Scientific, Logan, UT, USA) and a cavity-ring down absorption spectroscope (Picarro, Sunnyvale, CA, USA) as described previously (Ubierna *et al* ., 2017). The entire LI6400XT, the 2 cm x 6 cm leaf chamber (6400-11, Li-Cor), and LI-6400-18-RGB light source were placed in a growth cabinet (model EF7, Conviron; Controlled Environments Inc., MN, USA) with fluorescent lamps (F48T12/CW/ VHO; Sylvania, Wilmington, MA, USA) set at a PPFD of ˜250 μmol photons m^{-2} s^{-1} and air temperature was maintained at 25 °C. In current study, g_m was estimated using the method described by Ogee*et al.* , (2018) as discussed in Pathare *et al* ., (2020). This method utilizes a newly developed model of C_4photosynthetic discrimination that provides an estimate of the isotopic equilibration between CO_2 and H_2O inside the leaf and g_m.

Measurement of structural and anatomical traits associated with g_m and K_{leaf}

Light and electron microscopy techniques were used to measure important structural and anatomical traits listed in Table 1. The details of sample preparation for light and electron microscopy and measurements were presented in Pathare *et al* ., (2020). Light microscopy images of leaf cross sections were used to measure average leaf thickness (calculated as average of maximum and minimum leaf thickness) , interveinal distance (IVD), vein-to-adaxial epidermis distance (VED_{ada}), vein-to-abaxial epidermis distance (VED_{aba}), average VED (calculated as (VED_{ada} + VED_{aba}) /2) and length of mesophyll cell walls exposed to intercellular air spaces (IAS) using 10-15 different fields of view for each leaf (n = 3 per species) taken at x 50 and x 100 magnifications. Portion of BS cell walls exposed to IAS (BS_{ias}) was calculated as a percentage from the total BS cell wall length. BS area ratio was calculated as a percentage using BS area and mesophyll area (BS area/ [BS area + Mesophyll area]) for each species (Griffiths *et al* ., 2013). The mesophyll surface area exposed to IAS per unit leaf area (S_{mes}) was calculated from measurements of total length of mesophyll cell walls exposed to IAS and width of section analyzed using equation from Evans *et al.,* (1994) with curvature correction factor (F) of 1.34. Mesophyll and BS cell wall thickness ($\mathrm{M_{CW}}$ and $\mathrm{BS_{CW}}$) was measured from TEM micrographs using at least 15 images for each leaf. Total leaf vein length per unit leaf area (VLA) was calculated from the total number of veins per section length and expressed per mm^2considering parallel venation in grasses.

Images of the adaxial and abaxial epidermal surfaces, captured on four leaves (each from a different replicate; $n = 4$) per species under the low-vacuum mode with a FEI Scanning Electron Microscope Quanta 200F (FEI Co., Field Emission Instruments), were used to measure the stomatal number on each surface of leaf and expressed per mm^2as adaxial stomatal density ($\mathrm{SD_{ada}}$) and abaxial stomatal density ($\mathrm{SD_{aba}}$). The SR was calculated as ratio of the SD on the adaxial and abaxial surfaces. The stomatal size for adaxial ($\mathrm{SS_{ada}}$) and abaxial ($\mathrm{SS_{aba}}$) stomata was calculated as guard cell length x guard cell widths, $\mathrm{\mu m}^2$.

Estimation of $\mathrm{K_{leaf}}$

We used the leaf anatomical traits IVD, VED and average leaf thickness ($\mathrm{T_L}$) to estimate leaf hydraulic conductance ($\mathrm{K_{leaf}}$). Specifically, the traits used to estimate $\mathrm{K_{leaf}}$ in current study along with path of $\mathrm{CO_2}$ and water inside the leaf are indicated in Fig. S1. These traits have been shown to influence $\mathrm{K_{leaf}}$ in diverse species (Brodribb *et al.* , 2007; Sack *et al.* , 2013; Buckley *et al.* , 2015). The $\mathrm{K_{leaf}}$ was estimated as described by de Boer *et al* ., (2016) based on the empirical expression for $\mathrm{K_{leaf}}$ given by Brodribb *et al* ., (2007) as:

$$K_{\mathrm{leaf}} = 12674 \bullet {l_{H2O}}^{-1.26} \qquad \text{(Eqn 1)}$$

where,

$$l_{H2O} = \tau\sqrt{{\mathrm{dm}_x}^2 + \ \mathrm{VED}^2} \qquad \text{(Eqn 2)}$$

and τ is the tortuosity of the flow path throught the leaf intererior and assumed to be π/2 (Brodribb and Field, 2010). Thedm_x is the longest horizontal distance between the vein terminals (equivalent to $\mathrm{IVD_{max}}$; Brodribb *et al* . 2007; Brodribb and Field, 2010), and VED is the average vein-to-epidermis distance. Here we use average VED since there was a linear 1:1 relationship between $\mathrm{VED_{aba}}$ and $\mathrm{VED_{ada}}$ across the 18 $\mathrm{C_4}$ grasses measured in current study (Fig. S3). The $\mathrm{IVD_{max}}$ was not directly measured but was estimated from the published relationship between $\mathrm{IVD_{max}}$ and VLA, which is $\mathrm{IVD_{max}} = 650/\mathrm{VLA}$ (Brodribb *et al* ., 2007) and our observed relationship between IVD and VLA, which is $\mathrm{IVD} = 988/\mathrm{VLA}$ (Fig. S2) to estimate $\mathrm{IVD_{max}}$ as, $\mathrm{IVD_{max}} = 0.657 \times \mathrm{IVD}$.

In order to include average leaf thickness ($\mathrm{T_L}$) along with IVD and VED in the estimates of K $_{\mathrm{leaf}}$, the geometric relationship in the model of Brodribb and Field (2010) was modified according to de Boer *et al* ., (2016). For this, VED was assumed to be equal to $\mathrm{T_L}/2$ as supported from data presented in Fig. S4 in which slope of relationship is about 1/2. For IVD the relationship with ratio IVD/VED was considered where $\mathrm{VED} = \mathrm{T_L}/2$, so that$\mathrm{IVD} = \frac{\mathrm{IVD}}{\mathrm{VED}} \bullet \frac{T_L}{2}$. Using these expressions, Eqn 2 becomes:

$$l_{H2O} = \frac{\pi}{2}\sqrt{\frac{{T_L}^2}{4} + \frac{(0.657)^2}{4} \bullet \left(\frac{\mathrm{IVD}}{\mathrm{VED}}\right)^2 \bullet {T_L}^2} \qquad \text{(Eqn 3)}$$

Therefore, K $_{\mathrm{leaf}}$ can be calculated by substituting Eqn 3 in Eqn 1:

$$K_{\mathrm{leaf}} = \frac{7174}{\left(\frac{{T_L}^2}{4} + \frac{(0.657)^2}{4} \bullet \left(\frac{\mathrm{IVD}}{\mathrm{VED}}\right)^2 \bullet {T_L}^2\right)^{0.63}} \qquad \text{(Eqn 4)}$$

Calculation of $\mathrm{g_{max}}$

Total maximum stomatal conductance to water vapor ($\mathrm{g_{max}}$) was calculated as the sum of the maximum conductance values for adaxial ($\mathrm{g_{max\text{-}ada}}$) and abaxial side ($\mathrm{g_{max\text{-}aba}}$), as given in Taylor *et al* ., (2012), based on the model of Brown & Escombe (1900) after Franks & Beerling (2009a). The equation used to calculate $\mathrm{g_{max\text{-}ada}}$and $\mathrm{g_{max\text{-}aba}}$ is:

$$g_i = \frac{d}{v} \bullet D \bullet \frac{a_{\max}}{l + \frac{\pi}{2} \bullet \sqrt{\frac{a_{\max}}{\pi}}} \text{(Eqn 5)}$$

where,

the subscript g_i indicates the maximum stomatal conductance to water vapor for adaxial side ($g_{\text{max-ada}}$, mol m^{-2} s^{-1}) or abaxial side ($g_{\text{max-aba}}$, mol $m^{-2}s^{-1}$), d (m^2s^{-1}) is the diffusivity of water in air at 25°C, v (m^3mol^{-1}) is the molar volume of air at 25°C, D (m^{-2}) is the stomatal density for adaxial or abaxial side, $a_{\max}$ is the maximum stomatal pore area predicted from its relationship with stomatal size and l is the depth of stomata assumed to be equal to the guard cell widths. Stomatal density and size were measured as mentioned in previous section.

Statistical analysis

Statistical analyses were performed using R software (version 3.5.2, R Foundation for Statistical Computing, Vienna, Austria). Regression analysis were performed, using the mean values of traits for each species, in order to examine the relationships between key variables of interest among the 18 C_4 grasses. Particularly, we investigated the relationships of leaf structural and anatomical traits associated with g_m and photosynthetic C-gain and K_{leaf} and transpirational water-loss with habitat MAP and MAT. One-way ANOVA with posthoc Tukey's test was used to examine differences in leaf-level physiological, structural, anatomical and biochemical traits among the 18 diverse C_4 grasses (Refer Table S2, S3 and Pathare *et al* ., 2020). For the one-way ANOVA, values of P [?] 0.05 were considered to be statistically significant. Results of one-way ANOVA for traits used in the current study are given in Table S2 and S3 in current manuscript and in Pathare*et al* ., 2020. In addition, we used a principal component analysis (PCA) to identify the major axes of variation among the important leaf-level traits associated with g_m and K_{leaf} (Table 1). The R package FACTOMINER (Le *et al.* , 2008) was used to perform PCA. Because the traits had different units, they were scaled to unit variance and zero mean using correlation matrix before the analysis. The first three principal components (PCs) had eigenvalues > 1 (Table S4) and were retained according to Kaiser's rule (Kaiser, 1960). For each trait, factor loadings > 0.5 in absolute value were considered important.

Results

Effects of habitat MAP and MAT on leaf-level traits of C_4 grasses

We investigated the relationship of leaf-level traits, affecting g_m and K_{leaf} and hence photosynthetic C-gain and transpirational water-loss respectively, with two main habitat climate variables- mean annual temperature (MAT) and mean annual precipitation (MAP). Anatomical traits associated with g_m and K_{leaf} that were measured in current study are shown in Fig. S1. Mean values along with SE for the leaf-level traits measured in the current study are given in Table S2 and Pathare *et al* ., 2020. Mean values along with SE for MAP and MAT are shown in Fig. S9. None of the measured photosynthetic C-gain or transpirational water-loss traits measured in current study related with MAT (Table 1). However, MAP showed a significant relationship with many important leaf-level traits associated with photosynthetic C-gain or transpirational water-loss (Table 1, Fig. S5, S6 and S7). Specifically, there was a significant negative relationship between MAP and S_{mes} (R^2 = -0.50, $P< 0.01$), S_c (R^2 = -0.60, $P < 0.001$), SD_{ada}(R^2 = -0.20, $P = 0.06$), SR (R^2 = -0.21, $P = 0.05$), g_{max} (R^2 = -0.24, $P = 0.04$), $g_{\text{max-ada}}$ (R^2 = -0.43,$P = 0.003$), N_{area} (R^2 = -0.21, $P = 0.05$), leaf thickness (R^2 = -0.35, $P = 0.037$), average VED (R^2 = -0.45, $P = 0.01$), VED_{ada}(R^2 = -0.45, $P = 0.01$) and BS_{CW} (R^2 = -0.39, $P = 0.021$). Whereas, there was a significant positive relationship between BS_{ias} and MAP (R^2 = 0.27,$P = 0.026$). We also investigated the relationship of functional traits like g_m and g_{sw} with MAP for the 18 C_4 grasses. There was no significant relationship between g_{sw} and MAP (Table 1). However, there was a strong negative relationship between g_m and MAP (R^2 = -0.43, $P = 0.015$), whereas K_{leaf} showed a marginally significant positive relationship with MAP (R^2 = 0.20, $P = 0.07$, Table 1).

Principal component analysis

A PCA, using MAP and leaf-level structural and anatomical traits associated with g_m and K_{leaf}, was performed. The first two major axes (PC1 and PC2) along with the average position of 18 C_4 grasses in PC1-PC2 space are shown in Fig. 1. The, first four axes with eigenvalues and scores are shown in Table S4. PC1 explained about 54.5 % of the total variation in the C_4 grasses. PC1 scaled positively with A_{net}/E, A_{net}, $g_{max\text{-}ada}$, g_m, SD_{ada}, S_{mes}, SR, N_{area}, IVD, leaf thickness and average VED but negatively with K_{leaf}, total VLA and BS_{ias}. Thus, PC1 delineated the C_4grasses into those which show traits associated with greater g_m and hence photosynthetic C-gain (higher score on PC1) from those which show traits associated with greater K_{leaf} and water-loss (lower score on PC1). PC2 explained about 15 % of the total variation and scaled positively with BS_{CW} and S_{mes} but negatively with BS area ratio, BS_{IAS} and A_{net}. Together, the first two major axes explained about 70% of the total variation observed in the C_4 grasses. PC3 explained 9% of total variation and scaled positively only with BS area ratio and negatively with A_{net}/E. PC4 explained 7.67% of total variation and scaled positively with SD_{ada}..

Relationships of leaf structural and anatomical traits

To complement the PCA, we further investigated the important trait-to-trait comparisons. Across all the C_4 grasses, g_m was positively related with leaf-level traits used to estimate K_{leaf}, that is, IVD ($R^2 = 0.18$, $P = 0.07$, Fig. 2a), leaf thickness ($R^2 = 0.45$, $P < 0.01$, Fig. 2b) and average VED ($R^2 = 0.44$, $P < 0.01$, Fig. 2c), but negatively related with K_{leaf} ($R^2 = -0.28$, $P = 0.028$, Fig. 2d). Similarly, A_{net} was positively related with IVD ($R^2 = 0.46$, $P = 0.01$, Fig. 3a), leaf thickness ($R^2 = 0.15$, $P = 0.1$, Fig. 3b) and average VED ($R^2 = 0.22$, $P = 0.05$, Fig. 3c), but negatively related with K_{leaf}($R^2 = -0.31$, $P = 0.016$, Fig. 3d). In our previous study on these C_4 grasses (Pathare *et al* ., 2020), we showed that g_m scaled positively with S_{mes} ($R^2 = 0.63$, $P < 0.001$, Fig. S8a), SD_{ada}($R^2 = 0.47$, $P = 0.01$, Fig. S8c), SR ($R^2 = 0.26$, $P = 0.04$, Fig. S8d) and A_{net} ($R^2 = 0.26$, $P = 0.03$, Fig. S8h), but showed no relationship with M_{CW}, SD_{aba} and g_{sw} (Fig. S8b,e and f). Alternatively, K_{leaf} estimated using anatomical traits in current study showed a significant negative relationship with all of the above leaf-level structural and anatomical traits positively associated with g_m. Specifically, K_{leaf}scaled negatively with S_{mes} ($R^2 = -0.30$, $P = 0.027$, Fig. 4a), SR ($R^2 = -0.50$, $P < 0.001$, Fig. 4b) and SD_{ada}($R^2 = -0.38$, $P = 0.005$, Fig. 4c). Furthermore, traits associated with gm like S_{mes}, SD_{ada} and SR scaled positively with traits used to estimate K_{leaf} like IVD, leaf thickness and VED (Fig. 1, Table S4). We also investigated the relationships of $g_m$and K_{leaf} with g_{max}, $g_{max\text{-}ada}$ and $g_{max\text{-}aba}$. Particularly, g_m showed a significant positive relationship with g_{max} ($R^2 = 0.30$, $P = 0.018$, Fig. 5a) and $g_{max\text{-}ada}$($R^2 = 0.43$, $P < 0.01$, Fig. 5b) but did not relate with $g_{max\text{-}aba}$ (Fig. S8g). Whereas, K_{leaf} showed a significant negative relationship with $g_{max\text{-}ada}$ ($R^2 = -0.27$, $P = 0.025$, Fig. 5d) but did not relate with g_{max} and $g_{max\text{-}aba}$.

Discussion

Using 18 diverse C_4 grasses grown under common growth conditions, we investigated the relationship of growth habitat MAP and MAT with leaf-level structural and anatomical traits associated with g_m and K_{leaf}, which in turn could influence photosynthetic C-gain and water-loss. Many of the measured traits correlated with MAP but not with MAT (Table 1), which supports the previous expectations that, precipitation may be more important than temperature in affecting trait variability and potentially diversification in the C_4 species (Edwards & Still, 2008; Osborne & Sack, 2012; Liu *et al.* , 2019). Furthermore, our study provides insights into the possible relationships between g_m and leaf anatomical traits related to K_{leaf} in diverse C_4 grasses and suggest that C_4 grasses adapted to lower MAP exhibited traits associated with greater g_m and lower K_{leaf}.

C_4 grasses adapted to low MAP show traits associated with greater g_m and photosynthetic C-gain

A maximum A_{net} for a given rate of transpirational water-loss, through coordination of leaf-level photosynthetic and hydraulic traits, will in part determine species WUE and fitness during adaptation to drier growth habitats. A key question posed by earlier studies is how species adapted to drier habitats maintain similar or even higher A_{net}, at a given g_{sw}, during periods of active photosynthesis than species from more humid habitats (Wright *et al.* , 2001; Reich *et al.* , 2003). A greater A_{net}, at a given g_{sw}, can be achieved by increasing g_m through selection for leaf mesophyll traits like S_{mes} and S_c (Ivanova*et al.* , 2018a; Ivanova *et al.* , 2018b). In the current study, greater values for mesophyll traits like S_{mes} and S_c (Table 1) were observed in C_4 grasses adapted to lower MAP, as shown recently for C_3 species (Ivanova *et al.* , 2018a; Ivanova *et al.* , 2018b). S_{mes} and S_c have been demonstrated to be important determinants of g_m in C_3 (Muir*et al.* , 2014; Peguero-Pina *et al.* , 2017) and C_4 species (Pathare *et al.* , 2020) . For C_4 species, S_{mes} is a more accurate determinant of g_m then S_c as the first site of CO_2 fixation is in mesophyll cytosol and not the mesophyll chloroplast (Barbour *et al.* , 2016; Pathare *et al.* , 2020). If all else remains constant, then a greater S_{mes} increases the number of parallel pathways for CO_2 diffusion inside leaves leading to higher g_m under high light and low water availability (Terashima *et al.* , 2001; Ivanova *et al.* , 2018a; Ivanova*et al.* , 2018b). Indeed, along with greater S_{mes}, we also observed greater values for g_m in the C_4 grasses adapted to low MAP (Table1). Our findings thus support the previous work on C_3 plants suggesting the importance of mesophyll traits for plants adapted to drier habitats (Ivanova *et al.* , 2018b). Also, for the first time we show that C_4 grasses adapted to low MAP also exhibit mesophyll traits that lead to greater g_m -an important trait that could help achieve greater A_{net} at a given g_{sw} (Flexas *et al.* , 2016; Cousins *et al.* , 2020; Pathare *et al.* , 2020).

In addition to greater g_m and S_{mes}, C_4 grasses adapted to low MAP also showed greater SD_{ada}, g_{max}, SR and N_{area} (Table 1). Species adapted to conditions with high CO_2 demand, like high light and low water, have been shown to exhibit greater SD_{ada} and SR which may help decrease the effective leaf thickness and hence CO_2diffusion pathlength thus increasing g_m and supporting higher A_{net} (Parkhurst, 1978; Mott & O'Leary, 1984; Muir, 2018). We recently demonstrated that greater $SD_{ada}$and SR in C_4 grasses were associated with greater leaf thickness and lead to greater g_m and A_{net} as a result of increase in S_{mes}(Pathare *et al.* , 2020) . The current study further supports the well-established positive link of SD_{ada} and SR with habitat MAP (Mott & O'Leary, 1984; Bucher *et al.* , 2017) and suggests that a greater SD_{ada} and SR in drier habitats could be a strategy used by C_4 grasses to facilitate greater g_m and A_{net}. C_4grasses adapted to drier habitats also exhibited greater g_{max} (Table 1), which could enhance the capacity of C_4 grasses to achieve higher A_{net} in the shorter periods when water is available (Franks & Beerling, 2009).

C_4 grasses adapted to low MAP show leaf anatomical traits associated with lower K_{leaf} and transpirational water-loss

Our results demonstrate that C_4 grasses adapted to low MAP show greater g_m and associated traits like S_{mes}, S_c, SD_{ada}, SR and g_{max}, thus supporting the first hypothesis. However, these traits have also been associated with greater K_{leaf} in C_3 species (Brodribb & Holbrook, 2004; Xiong *et al.* , 2017; Drake *et al.* , 2019), which could imply higher water costs in drier habitats. However, C_4 grasses adapted to low MAP also showed greater leaf thickness and VED (Table 1), which indicates deeper vein placement and an increase in pathway for water movement outside the xylem (Brodribb*et al.* , 2007; McKown *et al.* , 2014; Buckley *et al.* , 2015). Additionally, in these C_4 grasses, an increase in leaf thickness was correlated with an increase in IVD i.e. a decrease in total VLA (Table 1). This may reduce the parallel water flow pathways outside xylem thus decreasing K_{ox} and hence K_{leaf} (Buckley *et al.* , 2015). Together, these anatomical traits suggest that K_{leaf} would be lower in C_4 grasses adapted to low MAP. Indeed, K_{leaf}, estimated using leaf thickness and VED, tended to be lower in C_4 grasses adapted to low MAP (Table 1). Furthermore, species adapted to low MAP also showed lower BS_{ias} and higher BS_{CW}-traits that may lower K_{ox} and hence K_{leaf} (Griffiths*et al.* , 2013; Buckley *et al.* , 2015; Scoffoni *et al.* , 2017). In summary, though C_4 grasses adapted to habitats with relatively low MAP exhibit traits associated with greater g_m and photosynthetic C-gain, they also possess traits associated with lower K_{leaf} and water-loss. This supports our second hypothesis as well as the previous expectation of selection for traits associated with lower K_{leaf} in C_4 species during adaptation to drier conditions (Zhou*et al.* , 2018). Thus, C_4 grasses from drier habitats can achieve greater photosynthetic C-gain at a given water-loss compared to C_4 grasses from relatively wet habitats.

Coordination of traits associated with $g_m$and K_{leaf}

Our findings on the coordination of traits associated with photosynthetic C-gain and transpirational water-loss in C_4 grasses contrast some of those reported previously for C_3 species. For instance, C_4 grasses adapted to drier habitats exhibit traits associated with greater g_m and lower K_{leaf} (Table 1). Also, g_m, A_{net} and traits associated with g_m like SD_{ada}, SR and S_{mes} (Pathare *et al* ., 2020) scaled positively with traits like IVD, leaf thickness and VED (Fig. 1) which are known to be important determinants of K_{leaf} (Sack *et al.* , 2013; Buckley *et al.* , 2015) These results suggest that K_{leaf} may be negatively related to $g_m$and hence A_{net} for the C_4 grasses belonging to habitats with diverse MAP. Indeed, K_{leaf}estimated using anatomical traits scaled negatively with g_m and A_{net}. This finding contrasts the previous reports of a positive relationship of $K_{leaf}$with g_m and A_{net} observed in C_3 species (Sack & Holbrook, 2006; Flexas *et al.* , 2013; Xiong *et al.* , 2017; Drake *et al.* , 2019) and could be partly explained by the carbon concentrating mechanism of C_4 species that maintains high A_{net} at relatively low g_{sw} compared to C_3species (Ocheltree *et al.* , 2016) and the relationship of g_m and K_{leaf} with leaf thickness. Specifically, greater leaf thickness in C_4 grasses from drier habitats was associated with greater VED and lower total VLA (Fig. 1) which may imply a lower K_{leaf} and also an increase in space available for photosynthetic tissue (Brodribb *et al.* , 2007; McKown *et al.* , 2014; Zwieniecki & Boyce, 2014; Buckley *et al.* , 2015). Also, in these C_4 grasses, greater leaf thickness was associated with a greater SD_{ada}, SR and S_{mes} implying a greater g_m and A_{net} (Muir, 2018). Consequently, we observed a negative relationship of K_{leaf} with g_m and hence A_{net} in these C_4 grasses. The negative relationship of SD_{ada} with total VLA and K_{leaf} (Fig. 1) also contrasts the previous reports for C_3 species (Drake *et al* ., 2019) and suggests that, for the C_4 grasses the presence of a greater number of stomata may not be associated with greater investment in leaf water transport tissue and hence K_{leaf} , though it is associated with a greater g_m and A_{net}(Pathare *et al* ., 2020).

Species adapted to drier habitats are known to employ a safer xylem strategy, wherein, resistance to cavitation is achieved by maintaining lower K_{leaf}, which however comes at the cost of A_{net} thus leading to the safety versus efficiency trade-off (Zimmermann, 1983; Meinzer *et al.* , 2010). However, C_4 grasses adapted to low MAP exhibited traits associated with lower K_{leaf}, but greater g_m and A_{net} (Table 1, Fig. 1). Previous studies have also observed a decoupling between $K_{leaf}$and A_{net} for the C_4 grasses (Kocacinar & Sage, 2003; Ocheltree *et al.* , 2016). Our results along with these previous findings suggest that maintaining a greater K_{leaf} in order to achieve greater A_{net}may not be a necessity for C_4 grasses and that the safety-versus efficiency trade-off may not apply to the C_4 grasses which can achieve greater $g_m$and A_{net} in drier habitats whilst maintaining a lower K_{leaf}.

The K_{leaf} values estimated here (10 to 27 mmol m^{-2} s^{-1} MPa^{-1}) using anatomical traits, are within the range measured previously (5 to 30 mmol m^{-2} s^{-1}MPa^{-1}) for diverse C_4 grasses (Liu & Osborne, 2015; Liu *et al.* , 2019). Because $K_{leaf}$was not measured directly, but estimated using a semi-empirical model based on diverse plant groups (Brodribb *et al.* , 2007; de Boer*et al.* , 2016), there are some uncertainties associated with using this model for C_4 grasses. For instance, the presence of Kranz anatomy, presence or absence of bundle-sheath suberisation and the relationship of stomatal density with VLA (Fig.1) can all influence the estimates of K_{leaf}. There is a need to address these uncertainties in future efforts for estimating K_{leaf} in C_4 grasses. Though we investigated the relationship of K_{leaf} with g_m and important mesophyll and BS traits, studies suggest that these traits may correlate strongly with the K_{ox} component of K_{leaf}, then K_x (Sack & Scoffoni, 2013; Buckley *et al.* , 2015). Investigating the relationship of g_m with K_{ox}, once a direct method for estimating K_{ox} is developed (Song & Barbour, 2016; Barbour, 2017; Barbour *et al.* , 2017), will provide greater ability to scale up from physiological processes to whole-leaf functions.

Conclusions

Leaf adaptation to climate may not be limited to a single or even a few traits but to a suite of traits representing a meaningful ‘syndrome’ that may be helpful for understanding vegetation response to climate change without detailed analysis of each species (Wright *et al.* , 2001; Reich *et al.* , 2003). Our results suggest that C_4 grasses adapted to low MAP exhibit greater SD_{ada}, SR, g_{max}, $S_{mes}$and g_m, which allow for greater photosynthetic C-gain and leaf-level WUE. Additionally, C_4 grasses adapted to low MAP also exhibit greater average leaf thickness, average VED and BS_{CW} but lower BS_{ias} which may lead to lower K_{leaf} and transpirational water-loss. This ‘syndrome’ of C_4 grasses appears important for adaptation to drier habitats and could be useful to identify or screen for agriculturally important C_4 grasses with greater productivities and leaf-level WUE (Sack *et al.* , 2016). Furthermore, a negative relationship of K_{leaf} with g_m, reported in current study for C_4grasses belonging to habitats with diverse MAP, warrants further investigation as it could have important implications for modelling the carbon and water fluxes of grasslands (De Kauwe *et al.* , 2015; Knauer *et al.* , 2019a; Knauer *et al.* , 2019b).

Acknowledgements

This work was supported by the Division of Chemical Sciences, Geosciences, and Biosciences, Office of Basic Energy Sciences, Department of Energy (grant no. DE-SC0001685) and the National Science Foundation (Major Research Instrumentation grant no. 0923562). We are grateful to Nerea Ubierna and Joseph Crawford for their valuable inputs on methods of estimation of mesophyll conductance in C_4species. We are also grateful to the Core Facility Center "Cell and Molecular Technologies in Plant Science" of Komarov Botanical Institute (St.-Petersburg, Russia) and Franceschi Microscopy and Imaging Center at Washington State University (Pullman, USA) for the use of its facilities and staff assistance. We would also like to thank Charles A. Cody for help in plant growth management.

Author contributions

V.S.P, B.V.S and A.B.C designed the experiment. V.S.P, B.V.S and N.K. performed the measurements and analyzed the data. V.S.P, B. V. S, N.K. and A.B.C interpreted the data. V.S.P led the writing with constructive inputs from B. V. S, N.K. and A.B.C.

Conflict of interest

The authors declare that they have no conflict of interest

References

Barbour MM. 2017. Understanding regulation of leaf internal carbon and water transport using online stable isotope techniques.*New Phytologist* **213** (1): 83-88.

Barbour MM, Evans JR, Simonin KA, von Caemmerer S. 2016. Online CO_2 and H_2O oxygen isotope fractionation allows estimation of mesophyll conductance in C_4 plants, and reveals that mesophyll conductance decreases as leaves age in both C_4 and C_3 plants. *New Phytologist***210** (3): 875-889.

Barbour MM, Farquhar GD, Buckley TN. 2017. Leaf water stable isotopes and water transport outside the xylem. *Plant Cell Environ* **40** (6): 914-920.

Brodribb TJ, Feild TS. 2010. Leaf hydraulic evolution led a surge in leaf photosynthetic capacity during early angiosperm diversification. *Ecol Lett* **13** (2): 175-183.

Brodribb TJ, Feild TS, Jordan GJ. 2007. Leaf maximum photosynthetic rate and venation are linked by hydraulics. *Plant Physiology* **144** (4): 1890-1898.

Brodribb TJ, Holbrook NM. 2004. Stomatal protection against hydraulic failure: a comparison of coexisting ferns and angiosperms.*New Phytologist* **162** (3): 663-670.

Bucher SF, Auerswald K, Grun-Wenzel C, Higgins SI, Garcia Jorge J, Romermann C. 2017. Stomatal traits relate to habitat preferences of herbaceous species in a temperate climate. *Flora* **229** : 107-115.

Buckley TN. 2015. The contributions of apoplastic, symplastic and gas phase pathways for water transport outside the bundle sheath in leaves. *Plant, Cell and Environment* **38** (1): 7-22.

Buckley TN, John GP, Scoffoni C, Sack L. 2015. How does leaf anatomy influence water transport outside the xylem? *Plant Physiology* **168** (4): 1616-1635.

Caringella MA, Bongers FJ, Sack L. 2015. Leaf hydraulic conductance varies with vein anatomy across *Arabidopsis thaliana*wild-type and leaf vein mutants. *Plant, Cell and Environment***38** (12): 2735-2746.

Christin P-A, Osborne CP, Chatelet DS, Columbus JT, Besnard G, Hodkinson TR, Garrison LM, Vorontsova MS, Edwards EJ. 2013. Anatomical enablers and the evolution of C_4 photosynthesis in grasses. *Proceedings of the National Academy of Sciences***110** (4): 1381-1386.

Cousins AB, Mullendore DL, Sonawane BV. 2020. Recent developments in mesophyll conductance in C_3, C_4, and crassulacean acid metabolism plants. *The Plant Journal* .

de Boer HJ, Drake PL, Wendt E, Price CA, Schulze E-D, Turner NC, Nicolle D, Veneklaas EJ. 2016. Apparent overinvestment in leaf venation relaxes leaf morphological constraints on photosynthesis in arid habitats. *Plant Physiology* **172** (4): 2286-2299.

De Kauwe MG, Zhou SX, Medlyn BE, Pitman AJ, Wang YP, Duursma RA, Prentice IC. 2015. Do land surface models need to include differential plant species responses to drought? Examining model predictions across a mesic-xeric gradient in Europe. *Biogeosciences* **12** (24): 7503-7518.

Drake PL, de Boer HJ, Schymanski SJ, Veneklaas EJ. 2019. Two sides to every leaf: water and CO_2 transport in hypostomatous and amphistomatous leaves. *New Phytologist***222** : 1179-1187.

Edwards EJ, Smith SA. 2010. Phylogenetic analyses reveal the shady history of C_4 grasses. *Proceedings of the National Academy of Sciences* **107** (6): 2532-2537.

Edwards EJ, Still CJ. 2008. Climate, phylogeny and the ecological distribution of C_4 grasses. *Ecol Lett***11** (3): 266-276.

Evans JR, Kaldenhoff R, Genty B, Terashima I. 2009. Resistances along the CO_2 diffusion pathway inside leaves.*Journal of Experimental Botany* **60** (8): 2235-2248.

Flexas J, Diaz-Espejo A, Conesa MA, Coopman RE, Douthe C, Gago J, Galle A, Galmes J, Medrano H, Ribas-Carbo M, et al. 2016. Mesophyll conductance to CO_2 and Rubisco as targets for improving intrinsic water use efficiency in C_3 plants.*Plant, Cell and Environment* **39** (5): 965-982.

Flexas J, Ribas-CarbO M, Diaz-Espejo A, GalmES J, Medrano H. 2008. Mesophyll conductance to CO_2: current knowledge and future prospects. *Plant, Cell and Environment* **31** (5): 602-621.

Flexas J, Scoffoni C, Gago J, Sack L. 2013. Leaf mesophyll conductance and leaf hydraulic conductance: an introduction to their measurement and coordination. *Journal of Experimental Botany***64** (13): 3965-3981.

Franks PJ, Beerling DJ. 2009. Maximum leaf conductance driven by CO_2 effects on stomatal size and density over geologic time. *Proceedings of the National Academy of Sciences***106** (25): 10343-10347.

Galmes J, Flexas J, Medrano H, Niinemets U, Valladares F 2012. Ecophysiology of photosynthesis in semi-arid environments.*Terrestrial Photosynthesis in a Changing Environment* : Cambridge University Press, Cambridge, UK., 448-464.

Griffiths H, Weller G, Toy LFM, Dennis RJ. 2013. You're so vein: bundle sheath physiology, phylogeny and evolution in C_3 and C_4 plants. *Plant, Cell and Environment* **36** (2): 249-261.

Hetherington AM, Woodward FI. 2003. The role of stomata in sensing and driving environmental change. *Nature***424** (6951): 901-908.

Hijmans R, van Etten J. 2012. Geographic analysis and modeling with raster data. *R package version* **2** : 1-25.

Ivanova LA, Ivanov LA, Ronzhina DA, Yudina PK, Migalina SV, Shinehuu T, Tserenkhand G, Voronin PY, Anenkhonov OA, Bazha SN, et al. 2018a. Leaf traits of C_3- and C_4-plants indicating climatic adaptation along a latitudinal gradient in Southern Siberia and Mongolia. *Flora* .

Ivanova LA, Yudina PK, Ronzhina DA, Ivanov LA, Holzel N. 2018b. Quantitative mesophyll parameters rather than whole-leaf traits predict response of C_3 steppe plants to aridity. *New Phytologist* **217** (2): 558-570.

Kaiser HF. 1960. The application of electronic computers to factor analysis. *Educational and Psychological Measurement* **20** (1): 141-151.

Knauer J, Zaehle S, De Kauwe MG, Bahar NHA, Evans JR, Medlyn BE, Reichstein M, Werner C. 2019a. Effects of mesophyll conductance on vegetation responses to elevated CO_2 concentrations in a land surface model. *Global Change Biology* **25** (5): 1820-1838.

Knauer J, Zaehle S, De Kauwe MG, Haverd V, Reichstein M, Sun Y. 2019b. Mesophyll conductance in land surface models: Effects on photosynthesis and transpiration. *The Plant Journal* .

Kocacinar F, Sage RF. 2003. Photosynthetic pathway alters xylem structure and hydraulic function in herbaceous plants. *Plant, Cell and Environment* **26** (12): 2015-2026.

Le S, Josse J, Husson F. 2008. FactoMineR: an R package for multivariate analysis. *Journal of Statistical Software* **25** (1): 1-18.

Liu H, Osborne CP. 2015. Water relations traits of C_4 grasses depend on phylogenetic lineage, photosynthetic pathway, and habitat water availability. *Journal of Experimental Botany* **66** (3): 761-773.

Liu H, Taylor SH, Xu Q, Lin Y, Hou H, Wu G, Ye Q. 2019. Life history is a key factor explaining functional trait diversity among subtropical grasses, and its influence differs between C_3 and C_4 species. *Journal of Experimental Botany* **70** (5): 1567-1580.

Loucos KE, Simonin KA, Barbour MM. 2017. Leaf hydraulic conductance and mesophyll conductance are not closely related within a single species. *Plant, Cell and Environment* **40** (2): 203-215.

McKown AD, Guy RD, Quamme L, Klapste J, La Mantia J, Constabel CP, El-Kassaby YA, Hamelin RC, Zifkin M, Azam MS. 2014. Association genetics, geography and ecophysiology link stomatal patterning in *Populus trichocarpa* with carbon gain and disease resistance trade-offs. *Mol Ecol* **23** (23): 5771-5790.

Meinzer FC, McCulloh KA, Lachenbruch B, Woodruff DR, Johnson DM. 2010. The blind men and the elephant: the impact of context and scale in evaluating conflicts between plant hydraulic safety and efficiency. *Oecologia* **164** (2): 287-296.

Mott KA, O'Leary JW. 1984. Stomatal behavior and CO_2 exchange characteristics in amphistomatous leaves. *Plant Physiology* **74** (1): 47-51.

Muir CD. 2018. Light and growth form interact to shape stomatal ratio among British angiosperms. *New Phytologist* **218** (1): 242-252.

Muir CD. 2019. Is amphistomy an adaptation to high light? Optimality models of stomatal traits along light gradients. *Integrative and Comparative Biology* **59** (3): 571-584.

Muir CD, Hangarter RP, Moyle LC, Davis PA. 2014. Morphological and anatomical determinants of mesophyll conductance in wild relatives of tomato (*Solanum* sect. *Lycopersicon* , sect. *Lycopersicoides* ; Solanaceae). *Plant, Cell and Environment* **37** (6): 1415-1426.

Nardini A, Luglio J. 2014. Leaf hydraulic capacity and drought vulnerability: possible trade-offs and correlations with climate across three major biomes. *Functional Ecology* **28** (4): 810-818.

Noblin X, Mahadevan L, Coomaraswamy IA, Weitz DA, Holbrook NM, Zwieniecki MA. 2008. Optimal vein density in artificial and real leaves. *Proceedings of the National Academy of Sciences* **105** (27): 9140-9144.

Ocheltree TW, Nippert JB, Prasad PVV. 2016. A safety *vs* efficiency trade-off identified in the hydraulic pathway of grass leaves is decoupled from photosynthesis, stomatal conductance and precipitation. *New Phytologist* **210** (1): 97-107.

Ogee J, Wingate L, Genty B. 2018. Mesophyll conductance from measurements of $C^{18}OO$ photosynthetic discrimination and carbonic anhydrase activity. *Plant Physiology* **178** : 728-752.

Osborne CP, Sack L. 2012. Evolution of C_4plants: a new hypothesis for an interaction of CO_2 and water relations mediated by plant hydraulics. *Philosophical Transactions of the Royal Society B: Biological Sciences***367** (1588): 583-600.

Parkhurst DF. 1978. The adaptive significance of stomatal occurrence on one or both surfaces of leaves. *Journal of Ecology***66** (2): 367-383.

Pathare VS, Koteyeva N, Cousins AB. 2020. Increased adaxial stomatal density is associated with greater mesophyll surface area exposed to intercellular air spaces and mesophyll conductance in diverse C4 grasses. *New Phytologist* **225** (1): 169-182.

Pearcy RW, Ehleringer J. 1984. Comparative ecophysiology of C_3 and C_4 plants. *Plant, Cell and Environment* **7** (1): 1-13.

Peguero-Pina JJ, Siso S, Flexas J, Galmes J, Garcia-Nogales A, Niinemets U, Sancho-Knapik D, Saz MA, Gil-Pelegrin E. 2017. Cell-level anatomical characteristics explain high mesophyll conductance and photosynthetic capacity in sclerophyllous Mediterranean oaks. *New Phytologist* **214** (2): 585-596.

Reich PB, Wright IJ, Cavender, Bares J, Craine JM, Oleksyn J, Westoby M, Walters MB. 2003. The evolution of plant functional variation: traits, spectra, and strategies. *International Journal of Plant Sciences* **164** (S3): S143-S164.

Sack L, Ball MC, Brodersen C, Davis SD, Des Marais DL, Donovan LA, Givnish TJ, Hacke UG, Huxman T, Jansen S, et al. 2016. Plant hydraulics as a central hub integrating plant and ecosystem function: meeting report for 'Emerging Frontiers in Plant Hydraulics' (Washington, DC, May 2015). *Plant, Cell and Environment* **39** (9): 2085-2094.

Sack L, Holbrook NM. 2006. Leaf hydraulics. *The Annual Review of Plant Biology* **57** : 361-381.

Sack L, Scoffoni C. 2013. Leaf venation: structure, function, development, evolution, ecology and applications in the past, present and future. *New Phytologist* **198** (4): 983-1000.

Sack L, Scoffoni C, John GP, Poorter H, Mason CM, Mendez-Alonzo R, Donovan LA. 2013. How do leaf veins influence the worldwide leaf economic spectrum? Review and synthesis. *Journal of Experimental Botany* **64** (13): 4053-4080.

Scoffoni C, Albuquerque C, Brodersen CR, Townes SV, John GP, Bartlett MK, Buckley TN, McElrone AJ, Sack L. 2017. Outside-xylem vulnerability, not xylem embolism, controls leaf hydraulic decline during dehydration. *Plant Physiology* **173** (2): 1197-1210.

Scoffoni C, Albuquerque C, Cochard H, Buckley TN, Fletcher LR, Caringella MA, Bartlett M, Brodersen CR, Jansen S, McElrone AJ, et al. 2018. The causes of leaf hydraulic vulnerability and its influence on gas exchange in *Arabidopsis thaliana* . *Plant Physiology***178** (4): 1584-1601.

Scoffoni C, Chatelet DS, Pasquet-kok J, Rawls M, Donoghue MJ, Edwards EJ, Sack L. 2016. Hydraulic basis for the evolution of photosynthetic productivity. *Nat Plants* **2** : 16072.

Sinclair TR, Zwieniecki MA, Holbrook NM. 2008. Low leaf hydraulic conductance associated with drought tolerance in soybean.*Physiologia Plantarum* **132** (4): 446-451.

Song X, Barbour MM. 2016. Leaf water oxygen isotope measurement by direct equilibration. *New Phytologist* **211** (3): 1120-1128.

Taylor SH, Aspinwall MJ, Blackman CJ, Choat B, Tissue DT, Ghannoum O. 2018. CO_2 availability influences hydraulic function of C_3 and C_4 grass leaves.*Journal of Experimental Botany* **69** (10): 2731-2741.

Terashima I, Miyazawa S-I, Hanba YT. 2001. Why are sun leaves thicker than shade Leaves? — Consideration based on analyses of CO_2 diffusion in the leaf. *Journal of Plant Research* **114** (1): 93-105.

Theroux-Rancourt G, Ethier G, Pepin S. 2014. Threshold response of mesophyll CO_2 conductance to leaf hydraulics in highly transpiring hybrid poplar clones exposed to soil drying.*Journal of Experimental Botany* **65** (2): 741-753.

Ubierna N, Gandin A, Boyd RA, Cousins AB. 2017. Temperature response of mesophyll conductance in three C_4 species calculated with two methods: ^{18}O discrimination and*in vitro* V_{pmax}. *New Phytologist***214** (1): 66-80.

Visser V, Woodward FI, Freckleton RP, Osborne CP. 2012. Environmental factors determining the phylogenetic structure of C_4 grass communities. *Journal of Biogeography***39** (2): 232-246.

Wang X, Du T, Huang J, Peng S, Xiong D. 2018. Leaf hydraulic vulnerability triggers the decline in stomatal and mesophyll conductance during drought in rice. *Journal of Experimental Botany***69** (16): 4033-4045.

Wright IJ, Reich PB, Westoby M. 2001. Strategy shifts in leaf physiology, structure and nutrient content between species of high- and low-rainfall and high- and low-nutrient habitats. *Functional Ecology* **15** (4): 423-434.

Xiong D, Flexas J, Yu T, Peng S, Huang J. 2017. Leaf anatomy mediates coordination of leaf hydraulic conductance and mesophyll conductance to CO_2 in *Oryza* . *New Phytologist* **213** (2): 572-583.

Xiong D, Nadal M. 2019. Linking water relations and hydraulics with photosynthesis. *The Plant Journal* **n/a** (n/a).

Xiong D, Yu T, Zhang T, Li Y, Peng S, Huang J. 2015. Leaf hydraulic conductance is coordinated with leaf morpho-anatomical traits and nitrogen status in the genus Oryza. *Journal of Experimental Botany* **66** (3): 741-748.

Zhou H, Helliker BR, Huber M, Dicks A, Akcay E. 2018.C_4 photosynthesis and climate through the lens of optimality. *Proceedings of the National Academy of Sciences***115** (47): 12057-12062.

Zimmermann MH. 1983. *Xylem structure and the ascent of sap* : Springer-Verlag.

Zwieniecki MA, Boyce CK. 2014. Evolution of a unique anatomical precision in angiosperm leaf venation lifts constraints on vascular plant ecology. *Proceedings of the Royal Society B: Biological Sciences* **281** (1779): 20132829.

Figure legends

Figure 1. Principal component analysis biplot showing major axes of variation in important leaf-level physiological, structural and anatomical traits among18 diverse C_4 grasses. Eigenvalues and factor loadings for first three principal components (PCs) are shown in Supporting Information Table S4. The arrows are the vectors showing the correlation (across the C_4 grasses) between a trait and the PCs. The position of species in PC space is shown in blue circles. Points are mean values with *n* =3–6 per species (Mean +- SE values are given in Pathare *et al* ., 2020 and Table S2). Species names correspond to the description in Table S1. Total VLA, vein length per unit leaf area; BS_{ias}, BS exposed to intercellular air spaces; BS_{CW}, BS cell wall thickness; BS exposed to intercellular air spaces; BS area ratio (calculated as (BS area/ [BS area + Mesophyll area]); g_m, mesophyll conductance to CO_2diffusion estimated by Ogee *et al* . (2018); A_{net}, net photosynthetic rates; A_{net}/E, instantaneous water-use efficiency; SD_{ada}, adaxial stomatal density; S_{mes}, total mesophyll cell surface area exposed to intercellular air space per unit of leaf surface area; SR, stomatal ratio; $g_{\text{max-ada}}$, maximum stomatal conductance for adaxial side; N_{area}, leaf N content expressed on area basis; IVD, interveinal distance; VED, average vein-to-epidermis distance; K_{leaf}, leaf hydraulic conductance.

Figure 2. Relationship of mesophyll conductance (g $_{\mathrm{m}}$) with (a) interveinal distance (IVD), (b) leaf thickness, (c) average vein-to-epidermis distance (VED) and leaf hydraulic conductance (K_{leaf}) for the 18 C_4 grasses measured in current study. Numbers correspond to species listed in Table S1. Regression coefficient (R ^{2}) is shown when P [?] 0.001 (***),P [?] 0.01 (**), P [?] 0.05 (*) and P [?] 0.1 (+). Points are mean values with n = 3-6 per species (Mean +- SE values are given in Pathare *et al* ., 2020 and Table S2).

Figure 3. Relationship of net photosynthetic rates (A_{net}) with (a) interveinal distance (IVD), (b) leaf thickness, (c) average vein-to-epidermis distance (VED) and leaf hydraulic conductance (K_{leaf}) for the 18 C_4 grasses measured in current study. Numbers correspond to species listed in Table S1. Regression coefficient (R ^{2}) is shown when P [?] 0.001 (***),P [?] 0.01 (**), P [?] 0.05 (*) and P [?] 0.1 (+). Points are mean values with n = 3-6 per species (Mean +- SE values are given in Pathare *et al* ., 2020 and Table S2).

Figure 4 . Relationship of leaf hydraulic conductance (K_{leaf}) with (a) mesophyll surface area exposed to intercellular air spaces (S_{mes}), (b) ratio of adaxial to abaxial stomatal density (SR) (c) adaxial stomatal density (SD_{ada}), and (d) abaxial stomatal density (SD_{aba}) for the 18 C_4 grasses. Numbers correspond to species listed in Table S1. Regression coefficient (R ^{2}) is shown when P [?] 0.001 (***),P [?] 0.01 (**), P [?] 0.05 (*) and P [?] 0.1 (+). Points are mean values with n = 3-6 per species (Mean +- SE values are given in Pathare *et al* ., 2020 and Table S2).

Figure 5. Relationship of mesophyll conductance (g $_{\mathrm{m}}$) and leaf hydraulic conductance with (a,c) total maximum stomatal conductance to water vapor (g_{max}) and (b, d) maximum stomatal conductance to water vapor for adaxial side ($g_{\mathrm{max\text{-}ada}}$) for the 18 C_4 grasses measured in current study. Numbers correspond to species listed in Table S1. Regression coefficient (R ^{2}) is shown when$P$ [?] 0.001 (***), P [?] 0.01 (**), P [?] 0.05 (*) and$P$ [?] 0.1 (+). Points are mean values with n = 3-6 per species (Mean +- SE values are given in Pathare *et al* ., 2020 and Table S2).

Supporting information

Table S1 . 18 C_4 grasses, along with biochemical subtype and evolutionary lineage, used in the current study (Adapted from Pathare *et al* ., 2020).

Table S2 . Mean +- SE (n = 3 to 6) values along with the corresponding letters of post-hoc Tukey's test for important leaf level traits measured in 18 C_4 grasses.

Table S3 . Results of one-way ANOVA with species as main effects for the traits measured in 18 C_4 grasses.

Table S4 . Component loadings for important leaf level traits determined on 18 diverse C_4 grasses.

Fig. S1 Representation of the anatomical traits associated with mesophyll conductance to CO_2 (g_{m}) and leaf hydraulic conductance (K_{leaf}) measured in current study.

Figure S2 : Relationship between total vein length per unit leaf area (total VLA) and interveinal distance (IVD).

Figure S3: Relationship between abaxial and adaxial distance from vein to epidermis (VED) in C_4 grasses.

Figure S4 : Relationship between average vein to the epidermis distance and leaf thickness in C_4 grasses.

Figure S5. Relationship of mean annual precipitation with (a) mesophyll surface area exposed to intercellular air space (S_{mes}), (b) extent of S_{mes} covered by chloroplast (S_{c}), (c) mesophyll conductance (g_{m}), (d) mesophyll cell wall thickness (M_{CW}), (e) adaxial stomatal density (SD_{ada}), (f) abaxial stomatal density (SD_{aba}) and stomatal ratio (SR) for the 18 C_4 grasses.

Figure S6. Relationship of mean annual precipitation with (a) total maximum stomatal conductance to water vapor (g_{max}) , (b) maximum stomatal conductance to water vapor for adaxial side ($g_{\mathrm{max\text{-}ada}}$), (c) maximum stomatal conductance to water vapor for abaxial side ($g_{\mathrm{max\text{-}aba}}$), (d) N content per unit leaf area (N_{area}), (e) stomatal conductance to water (g_{sw}), (f) leaf thickness and (g) average vein to epidermis distance (VED) for the 18 C_4 grasses.

Figure S7. Relationship of mean annual precipitation with (a) vein to adaxial epidermis distance ($\mathrm{VED_{ada}}$), (b) vein to abaxial epidermis distance ($\mathrm{VED_{aba}}$), (c) interveinal distance (IVD), (d) Bundle sheath cell wall thickness ($\mathrm{BS_{CW}}$), (e) BS exposed to intercellular air space ($\mathrm{BS_{ias}}$), (f) BS area ratio (calculated as (BS area/ [BS area + Mesophyll area])) and (g) leaf hydraulic conductance ($\mathrm{K_{leaf}}$) for the 18 $\mathrm{C_4}$ grasses.

Figure S8. Relationship of mesophyll conductance to $\mathrm{CO_2}$ ($\mathrm{g_m}$) with (a) mesophyll surface area exposed to intercellular air spaces ($\mathrm{S_{mes}}$), (b) Mesophyll (M) cell wall thickness ($\mathrm{M_{CW}}$), (c) adaxial stomatal density ($\mathrm{SD_{ada}}$), (d) stomatal ratio or ratio of adaxial to abaxial stomatal density (SR), (e) abaxial stomatal density ($\mathrm{SD_{aba}}$), (f) stomatal conductance to water ($\mathrm{g_{sw}}$), (g) maximum stomatal conductance for abaxial side (gmax-aba) and (h) net $\mathrm{CO_2}$ assimilation rates ($\mathrm{A_{net}}$) for the 18 $\mathrm{C_4}$ grasses.

Figure S9. Boxplot showing habitat (a) mean annual precipitation and (b) mean annual temperature for 18 $\mathrm{C_4}$grasses measured in current study.

Table 1. Relations between habitat climate variables (MAP and MAT) and important anatomical, stomatal and functional traits associated with carbon gain and water use in 18 diverse $\mathrm{C_4}$ grasses.

Hosted file

`image1.emf` available at https://authorea.com/users/300599/articles/446753-c4-grasses-adapted-to-low-precipitation-habitats-show-traits-related-to-greater-mesophyll-conductance-and-lower-leaf-hydraulic-conductance

Regression coefficient (R^{2}), P -values and type of regression model fit are shown. $R^{2}$is shown in bold when P [?] 0.001 (***), P [?] 0.01 (**),P [?] 0.05 (*) and P [?] 0.1 (+). $\mathrm{S_{mes}}$, total mesophyll cell surface area exposed to intercellular air space per unit of leaf surface area; $\mathrm{S_c}$, chloroplast coverage of $\mathrm{S_{mes}}$, $\mathrm{g_m}$, mesophyll conductance to $\mathrm{CO_2}$ diffusion estimated by Ogee *et al* . (2018); mesophyll cell wall thickness ($\mathrm{M_{CW}}$); $\mathrm{SD_{ada}}$, adaxial stomatal density; $\mathrm{SD_{aba}}$, abaxial stomatal density; SR, stomatal ratio; $\mathrm{g_{max}}$, maximum stomatal conductance to water vapor; $\mathrm{g_{max\text{-}ada}}$, maximum stomatal conductance to water vapor for adaxial side; $\mathrm{g_{max\text{-}aba}}$, maximum stomatal conductance to water vapor for abaxial side; $\mathrm{N_{area}}$, leaf N content expressed on area basis; stomatal conductance to water vapor diffusion ($\mathrm{g_{sw}}$); VED, average vein-to-epidermis distance; $\mathrm{VED_{ada}}$, vein-to-adaxial epidermis distance; $\mathrm{VED_{aba}}$, vein-to-adaxial epidermis distance; IVD, interveinal distance; total VLA, vein length per unit leaf area; $\mathrm{BS_{CW}}$, BS cell wall thickness; $\mathrm{BS_{ias}}$, BS exposed to intercellular air spaces; BS area ratio (calculated as (BS area/ [BS area + Mesophyll area]); $\mathrm{K_{leaf}}$, leaf hydraulic conductance.

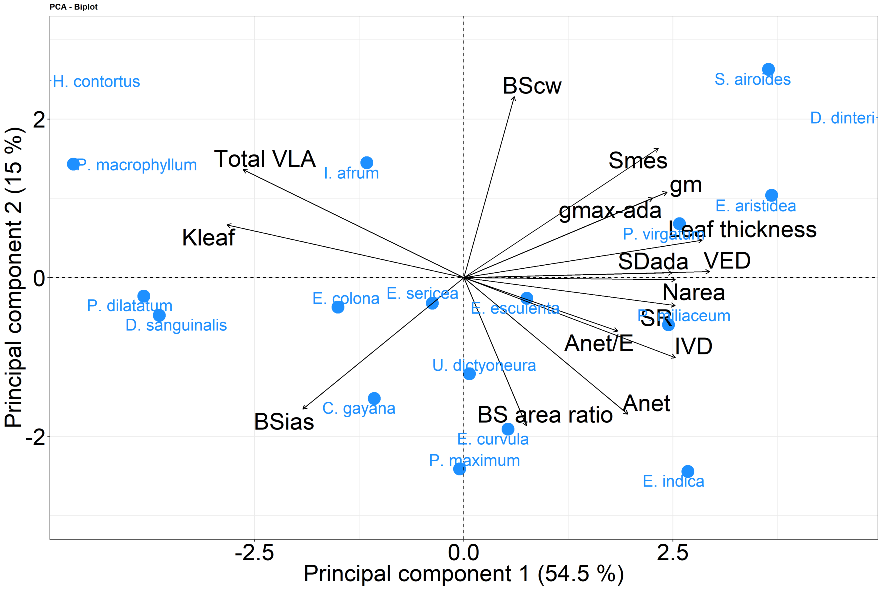

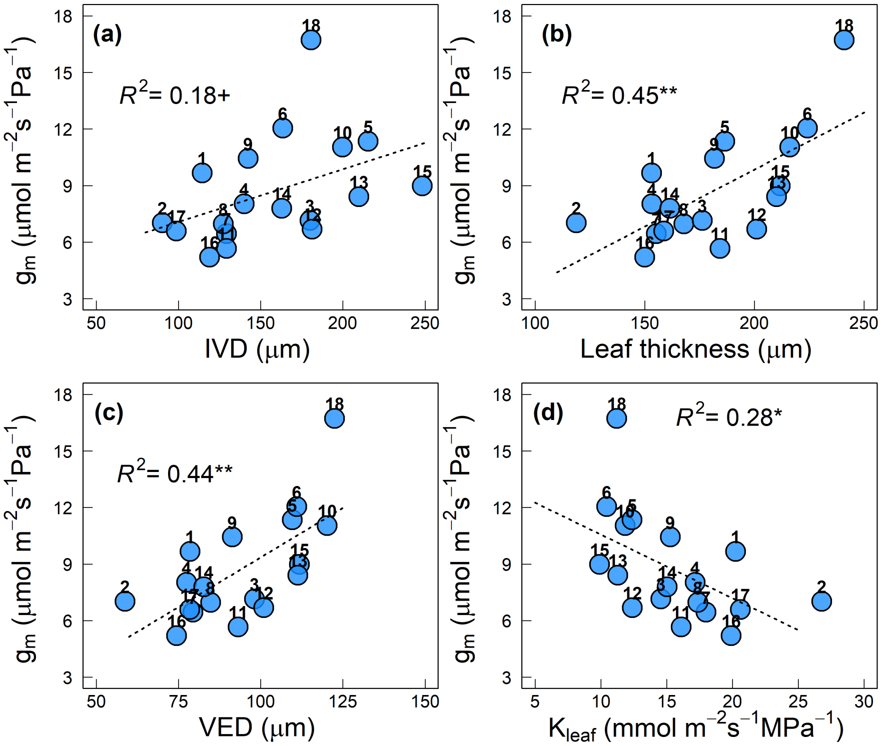
(a)
R^2= 0.18+
g_m (μmol m^{-2}s^{-1}Pa^{-1})
IVD (μm)
3 6 9 12 15 18
50 100 150 200 250
18 6 10 5 1 9 4 14 13 15 2 17 8 7 3 12 16 11
(b)
R^2= 0.45**
g_m (μmol m^{-2}s^{-1}Pa^{-1})
Leaf thickness (μm)
100 150 200 250
18 6 5 10 9 1 15 13 4 14 2 17 8 3 12 11 16
(c)
R^2= 0.44**
g_m (μmol m^{-2}s^{-1}Pa^{-1})
VED (μm)
50 75 100 125 150
18 6 5 10 1 9 15 13 4 14 2 17 8 3 12 16 11
(d)
R^2= 0.28*
g_m (μmol m^{-2}s^{-1}Pa^{-1})
K_{leaf} (mmol m^{-2}s^{-1}MPa^{-1})
5 10 15 20 25 30
18 6 5 10 9 1 15 13 14 4 3 8 12 17 2 7 11 16

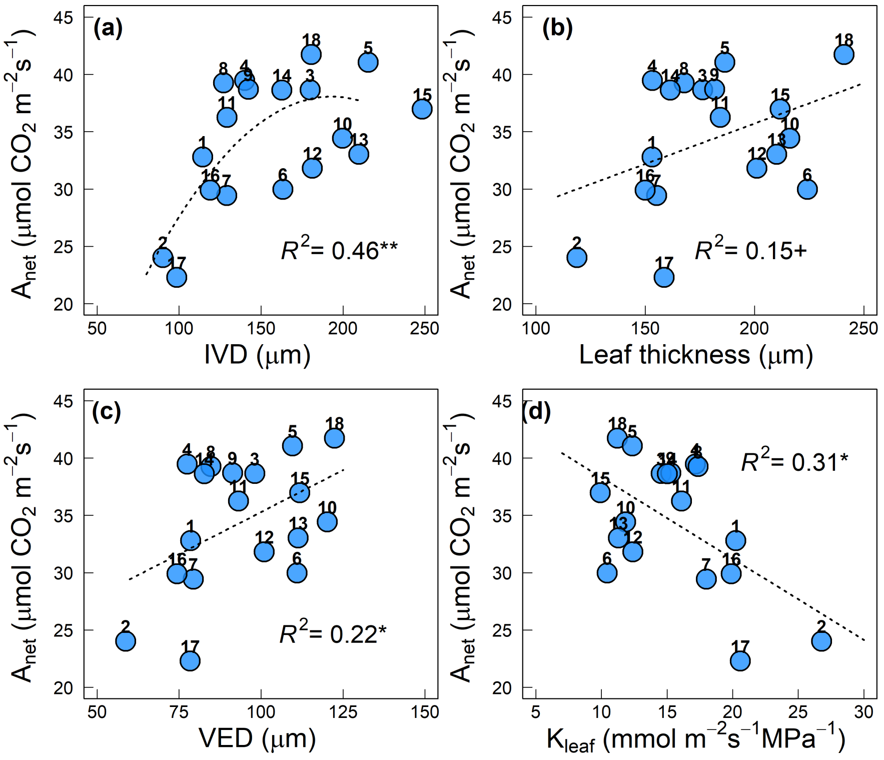
(a)
R^2= 0.46**
A_{net} (μmol CO$_2$ m^{-2}s^{-1})
IVD (μm)
20 25 30 35 40 45
50 100 150 200 250
18 5 8 4 9 14 3 15 11 10 13 1 12 16 7 6 2 17
(b)
R^2= 0.15+
A_{net} (μmol CO$_2$ m^{-2}s^{-1})
Leaf thickness (μm)
100 150 200 250
18 5 4 14 8 3 9 15 11 10 13 1 12 16 7 6 2 17
(c)
R^2= 0.22*
A_{net} (μmol CO$_2$ m^{-2}s^{-1})
VED (μm)
50 75 100 125 150
18 5 4 14 8 9 3 15 11 10 13 1 12 16 7 6 2 17
(d)
R^2= 0.31*
A_{net} (μmol CO$_2$ m^{-2}s^{-1})
K_{leaf} (mmol m^{-2}s^{-1}MPa^{-1})
5 10 15 20 25 30
18 5 15 11 4 8 10 13 12 1 6 7 16 2 17

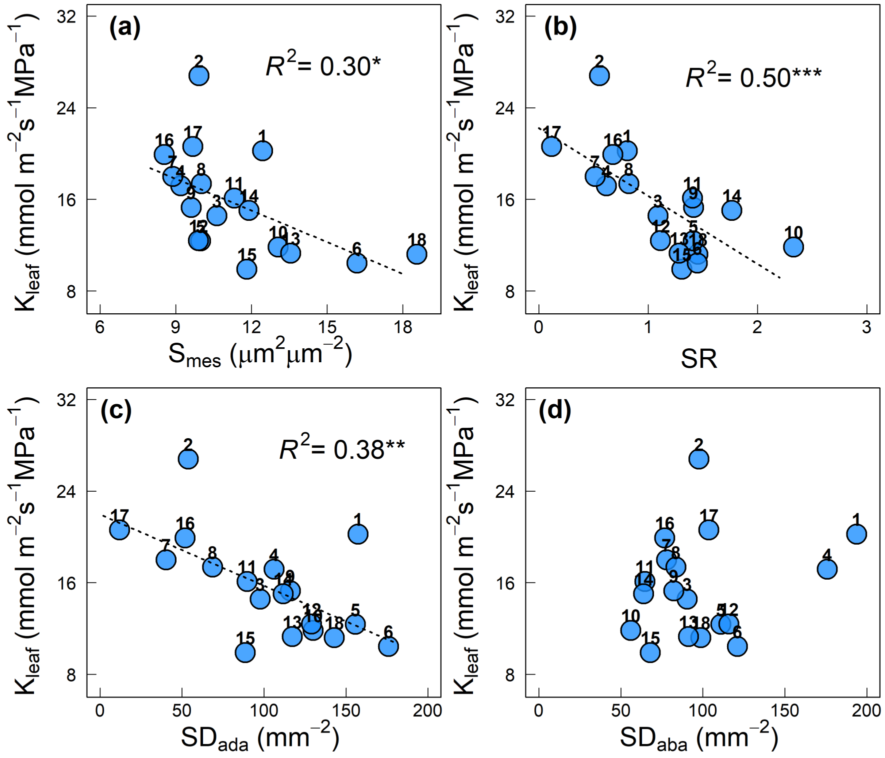
(a)
R^2= 0.30*
K_{leaf} (mmol m^{-2}s^{-1}MPa^{-1})
8
16
24
32
6
9
12
15
18
S_{mes} (µm^{2}µm^{-2})
(b)
R^2= 0.50***
0
1
2
3
SR
(c)
R^2= 0.38**
0
50
100
150
200
SD_{ada} (mm^{-2})
(d)
SD_{aba} (mm^{-2})

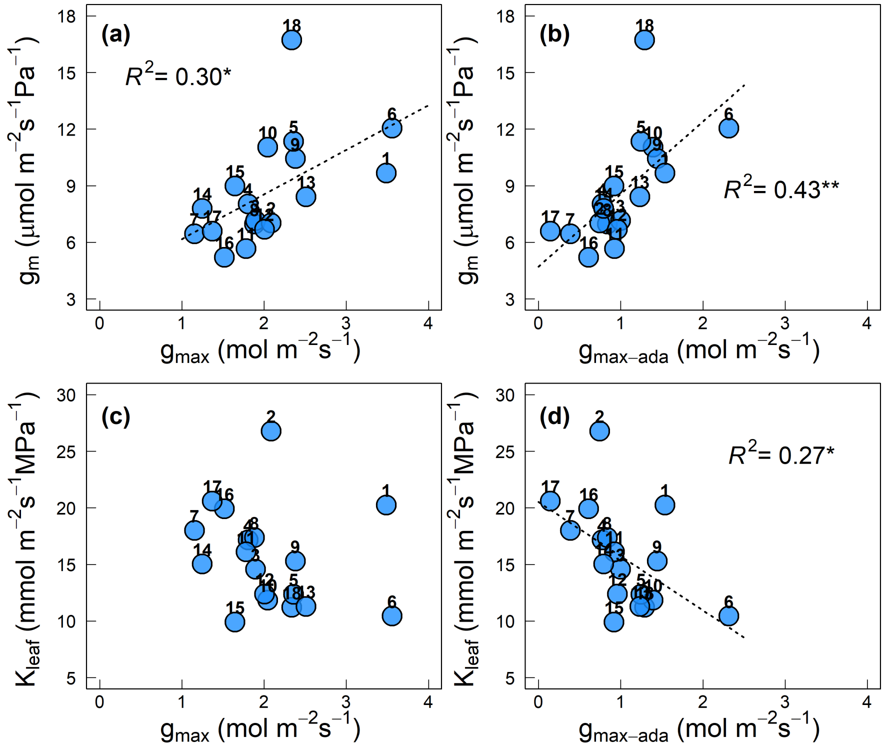
(a)
R^2= 0.30*
g_m (µmol m^{-2}s^{-1}Pa^{-1})
3
6
9
12
15
18
0
1
2
3
4
g_{max} (mol m^{-2}s^{-1})
(b)
R^2= 0.43**
$g_{max-ada}$ (mol m^{-2}s^{-1})
(c)
K_{leaf} (mmol m^{-2}s^{-1}MPa^{-1})
5
10
15
20
25
30
(d)
R^2= 0.27*